

Exploiting Constructive Interference for Backscatter Communication Systems

Bowen Gu, *Student Member, IEEE*, Dong Li, *Senior Member, IEEE*, Ye Liu, *Member, IEEE*, Yongjun Xu, *Senior Member, IEEE*

Abstract—Backscatter communication (BackCom), one of the core technologies to realize zero-power communication, is expected to be a pivotal paradigm for the next generation of the Internet of Things (IoT). However, the “strong” direct link (DL) interference (DLI) is traditionally assumed to be harmful, and generally drowns out the “weak” backscattered signals accordingly, thus deteriorating the performance of BackCom. In contrast to the previous efforts to eliminate the DLI, in this paper, we exploit the constructive interference (CI), in which the DLI contributes to the backscattered signal. To be specific, our objective is to maximize the received signal power by jointly optimizing the receive beamforming vectors and tag selection factors, which is, however, non-convex and difficult to solve due to constraints on the Kullback-Leibler (KL) divergence. In order to solve this problem, we first decompose the original problem, and then propose two algorithms to solve the sub-problem with beamforming design via a change of variables and semi-definite programming (SDP) and a greedy algorithm to solve the sub-problem with tag selection. In order to gain insight into the CI, we consider a special case with the single-antenna reader to reveal the channel angle between the backscattering link (BL) and the DL, in which the DLI will become constructive. Simulations results show that significant performance gain can always be achieved in the proposed algorithms compared with the traditional algorithms without the DL in terms of the strength of the received signal. The derived constructive channel angle for the BackCom system with the single-antenna reader is also confirmed by simulations results.

Index Terms—Backscatter communication, constructive interference, Kullback-Leibler divergence, tag selection

I. INTRODUCTION

As the number of connected devices has grown by leaps and bounds over the past few decades, the Internet of Things (IoT) is transforming industry, logistic, and everyday use in an unforeseen manner, ushering in a new industrial revolution [1], [2]. Recent market studies envision that the total number of connected IoT devices will reach 83 billion by 2024, rising from 35 billion connections in 2020 [3]. However, this is a mixed blessing, as further promotion of the IoT will necessitate a huge expense consumed to maintain these ever-

increasing devices’ operation. Recently, backscatter communication (BackCom) has been emerging as a promising technology that can break the gridlock of these power-hungry devices, which are replaced by passive tags without the need of active radio frequency (RF) components [4]. In the BackCom system, the externally generated carrier by a dedicated power source is utilized to carry the tag’s signal, and only the impedance loading is applied to backscatter the received signal, which can significantly reduce the hardware cost and pave the way for zero-power communication [5].

However, it should be noted that, in the BackCom system, the backscattered signal actually undergoes double-channel fading, which is to blame for the quite weak signal strength at the reader. It is extremely difficult to recover the backscattered data from different tags due to the mutual interference caused by the concurrent transmission [6]. On the other hand, another issue ensues: when the signal from the direct link (DL) encounters these weak signals at the reader, the resulting interference is strong enough to drown out the desired signal [7]. Therefore, it is hard to overstate the importance of interference suppression for BackComs.

In fact, interference suppression has been fruitfully studied in BackCom systems. One of the most typical methods is the successive interference cancellation (SIC) technique [8], [9], by which the strong interference signal in the mixed signal can be stripped. However, it has to be noted that the SIC may suffer from the residual interference, and interference cancellation for multiple weak signals may not perform well. In this regard, the frequency shift (FS) technique has been proposed as a promising method to mitigate the interference in BackCom systems [10]. To be specific, each backscatter tag can shift its carrier signal to adjacent non-overlapping frequency bands and isolate the backscattered signal from the DL signal so that the mutual interference between different tags and the DL interference (DLI) can be avoided [11]–[14]. Furthermore, BackCom systems over orthogonal frequency division multiplexing (OFDM) carriers are proposed in [15]–[17], which cancels out the DLI by exploiting the repeating structure of the ambient OFDM signals by the aid of the cyclic prefix. Besides, time division multiple access (TDMA) (see, [18]–[20]) and tag selection (see, [21]–[23]) are also widely used in BackCom systems to avoid the mutual interference among different tags.

A. Motivations and Contributions

It is noted that, most of the existing works assume that the DLI is always harmful, and thus focus on how to avoid

Bowen Gu and Dong Li are with the School of Computer Science and Engineering, Macau University of Science and Technology, Avenida Wai Long, Taipa, Macau 999078, China (e-mails: gubwww@163.com, dli@must.edu.mo).

Ye Li is with the College of Artificial Intelligence, Nanjing Agricultural University, Nanjing 210031, China, and also with the School of Computer Science and Engineering, Macau University of Science and Technology, Avenida Wai Long, Taipa, Macau 999078, China. (e-mail: yeliu@njau.edu.cn).

Yongjun Xu is with the School of Communication and Information Engineering, Chongqing University of Posts and Telecommunications, Chongqing 400065, China (e-mail: xuyj@cqupt.edu.cn).

the effects of interference for BackCom systems. However, there are several natural questions that arise: is interference necessarily destructive in all cases? is it possible to blaze a trail to turn the destructive interference into a constructive one? These problems have received little attention, and there have been only several research efforts paid to answer the above questions. The constructive interference (CI) was achieved among multiple cooperative tags in centralized scenarios [24] and decentralized scenarios [25], respectively, in which several tags backscatter the same packet synchronously which makes it possible that backscattered signals can be constructively combined, leading to an increased signal strength at the reader. Besides, a BackCom system with the symbol level precoding technique is proposed in [26] to convert the multi-user interference into the constructive region of the desired data symbol by designing the transmit beamforming on the symbol level.

Although the CI was considered in [24] and [25] among different tags in BackCom systems, which means that CI can be found among multiple weak signals, they ignore the real protagonist, namely, the strong interference from the DL, since compared with the mutual interference among tags, the DLI is more harmful. In [26], the multi-user interference in broadcasting channels was considered to be converted into the CI, where the tag signal detection is not taken into account and there is actually no DLI. In this regard, we take up the baton in this paper to probe how to convert the DLI into a helpful interference in enhancing the backscattered signal strength, which is in contrast to most of the existing works that aim at canceling the DLI [8]–[22]. To the best of our knowledge, this is the first attempt to harness the DLI for the backscattered signal for BackCom systems. To be specific, we consider the communication between a power source (PS) and a multi-antenna reader in the presence of multiple tags.

Specifically, the contributions of this paper are summarized as follows:

- To evaluate whether the DLI is constructive or not, a novel Kullback-Leibler divergence (KLD)-oriented approach is proposed, where the KLDs of the received signals with and without the DL are compared. By doing so, the CI can be obtained. However, the mutual interference among multiple tags also hinders the exploitation of the CI, and we consider tag selection to avoid this problem. It worth pointing out that the KLD analysis of the DLI is new, and not presently available in existing works.
- Our objective is to maximize the received power subjective to constraints on the CI and the minimum KLD via beamforming design and tag selection. However, the formulated problem is non-convex and hard to solve. In order to circumvent this difficulty, we first decompose the problem and then reformulate it via a change of variables. The resulting problem can be solved by the aid of the semi-definite programming (SDP) for beamforming design and greedy search for tag selection.
- In order to gain more insight into the CI, we consider a special case with one single antenna at the reader. In this case, we are able to derive a closed-form expression for the upper bound on the angle between the backscattering

TABLE I
ABBREVIATIONS

Notation	Meaning
BackCom	Backscatter communication
BER	Bit error rate
BL	Backscattering link
CI	Constructive interference
CSCG	Circularly symmetric complex Gaussian
DL	Direct link
DLI	Direct-link interference
FS	Frequency shift
KLD	Kullback-Leibler divergence
LCBA	Low complexity-based algorithm
OFDM	Orthogonal frequency division multiplexing
PDF	Probability density function
PS	Power source
RC	Reflection coefficient
RF	Radio frequency
SIC	Successive interference cancellation
SDP	Semi-definite programming
SIMO	Single input multiple output
SISO	Single input single output
SNR	Signal-to-noise ratio
TDMA	Time division multiple access
VRBA	Variable relaxation-based algorithm

link (BL) and the DL, where the CI exists. This result is new and unique in the sense of its potential to build up the CI in practice.

- Simulations results show that significant performance gain can be always achieved in the proposed algorithms compared with the benchmark algorithms in terms of the received signal power. Besides, the CI is demonstrated for the case with the multiple antennas at the reader, and the derived angle for the case with one single antenna at the reader is also confirmed by simulations results. Moreover, they also demonstrate from the derived angle that it is more likely to build up the CI for the relatively weak DLI or not sufficiently large input SNR.

B. Organization

The remainder of the paper is organized as follows: In Section II, we present the system model and analyze the KLDs for two different cases. In Section III, an optimization problem for maximizing the received signal power is formulated, and two algorithms are proposed to solve it. Besides, a special case is also considered for more insight in Section III. Section IV gives the simulation results, and Section V concludes this paper.

C. Notations

Throughout the paper, scalars, vectors, and matrices are denoted by lowercase, boldface lowercase, and boldface uppercase letters, respectively. $(\cdot)^H$, $|\cdot|$, $\|\cdot\|$, $\det(\cdot)$, $\text{Rank}(\cdot)$,

and $\text{Tr}(\cdot)$ represent the Hermitian, the absolute value, the l_2 norm, the determinant, the rank, and the trace of the matrix, respectively. $\mathcal{CN}(\mu, \sigma^2)$ is the circularly symmetric complex Gaussian (CSCG) distribution with mean μ and variance σ^2 . $\lambda^{\max}(\cdot)$ and $\lambda^{\min}(\cdot)$ denote the maximum eigenvalue of the matrix. \mathbf{I}_N represents the $N \times N$ identity matrix. $W_0(\cdot)$ and $W_{-1}(\cdot)$ denote the principal branch and the bottom branch of the Lambert W function, respectively. $\mathcal{O}(\cdot)$ is the big-O computational complexity notation. The abbreviations in this paper are given by Table I.

II. SYSTEM MODEL AND KLD ANALYSIS

A. System Model

We consider a BackCom system with single input multiple output (SIMO) as shown in Fig. 1, with a PS, K single-antenna tags ($k \in \mathcal{K} = \{1, 2, \dots, K\}$), and a common reader with M antennas ($m \in \mathcal{M} = \{1, 2, \dots, M\}$). The channel coefficients of the PS-tag k link, the PS-reader link, and the tag k -reader link are respectively given by $\mathbf{h}_{\text{ST}}^k \in \mathbb{C}^{1 \times 1}$, $\mathbf{h}_{\text{SR}} \in \mathbb{C}^{M \times 1}$, and $\mathbf{h}_{\text{TR}}^k \in \mathbb{C}^{M \times 1}$. Assume that channels between the transmitter and the receiver follow a block-fading based model, namely, \mathbf{h}_{ST}^k , \mathbf{h}_{SR} , and \mathbf{h}_{TR}^k remain constant during backscattering in one time interval, but vary independently in different intervals. It is further assumed that the PS transmits N CGCS signals $s(n)$, $n \in \mathcal{N} = \{1, 2, \dots, N\}$ with the transmitted power σ_s^2 in one time interval. Moreover, $s(n)$ for $n = \{1, 2, \dots, N\}$ are independent and identically distributed (i.i.d.). Then, the received signal $\mathbf{x}_k(n)$ at the reader can be expressed as

$$\mathbf{x}_k(n) = \underbrace{\mathbf{h}_{\text{SR}} s(n)}_{\text{Direct signal}} + \underbrace{\sqrt{\alpha_k} \beta_k \mathbf{h}_{\text{ST}}^k \mathbf{h}_{\text{TR}}^k s(n)}_{\text{Backscattering signal}} c_k(n) + \underbrace{\mathbf{w}(n)}_{\text{Noise}}, \quad (1)$$

where α_k is the reflection coefficient (RC) of the k -th tag. $\mathbf{w}(n) \in \mathbb{C}^{M \times 1}$ denotes the noise vector of the reader and is assumed to be an i.i.d. CSCG random vector with $\mathbf{w}(n) \sim \mathcal{CN}(0, \sigma_w^2 \mathbf{I}_M)$. σ_w^2 denotes the noise power. β_k is the tag selection factor, i.e., $\beta_k = 1$ denotes the k -th tag is selected, otherwise $\beta_k = 0$. Besides, $c_k(n) \in \{0, 1\}$ denotes the k -th tag's symbol with the binary on-off keying modulation, i.e., $c_k(n) = 0$ refers to that the k -th tag does not backscatter the RF source signal; otherwise, the k -th tag chooses to backscatter the RF source signal [27]. By using the receive beamforming, the received signal at the reader is

$$\begin{aligned} y_k(n) &= \mathbf{v}_k^H \mathbf{x}_k(n) \\ &= \mathbf{v}_k^H \mathbf{h}_{\text{SR}} s(n) + \sqrt{\alpha_k} \beta_k \mathbf{h}_{\text{ST}}^k \mathbf{v}_k^H \mathbf{h}_{\text{TR}}^k s(n) c_k(n) + \mathbf{v}_k^H \mathbf{w}(n), \end{aligned} \quad (2)$$

where $\mathbf{v}_k \in \mathbb{C}^{M \times 1}$ denotes the beamforming vector at the reader.

B. KLD Analysis

As mentioned earlier, we utilize the KLD to analyze the CI. Specifically, when the DL is available, the received signal of the reader can be rewritten with a binary hypothesis, i.e.,

$$y_k(n) = \begin{cases} \mathcal{H}_0 : \mathbf{v}_k^H \mathbf{h}_0 s(n) + \mathbf{v}_k^H \mathbf{w}(n), & c_k(n) = 0, \\ \mathcal{H}_1 : \mathbf{v}_k^H \mathbf{h}_1^k s(n) + \mathbf{v}_k^H \mathbf{w}(n), & c_k(n) = 1, \end{cases} \quad (3)$$

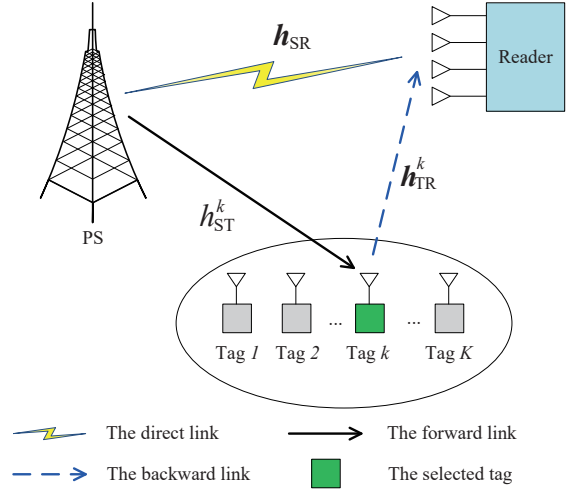


Fig. 1. A multi-tag SIMO-based BackCom system model.

where $\mathbf{h}_0 = \mathbf{h}_{\text{SR}}$, $\mathbf{h}_1^k = \mathbf{h}_{\text{SR}} + \mathbf{h}_{\text{STR}}^k$, and $\mathbf{h}_{\text{STR}}^k = \sqrt{\alpha_k} \beta_k \mathbf{h}_{\text{ST}}^k \mathbf{h}_{\text{TR}}^k$.

Thus, the distributions of the received signals $y_k(n)$ can be expressed as

$$\begin{cases} \mathcal{H}_0 : y_k(n) \sim \mathcal{CN}(0, \delta_0^k), & c_k(n) = 0, \\ \mathcal{H}_1 : y_k(n) \sim \mathcal{CN}(0, \delta_1^k), & c_k(n) = 1, \end{cases} \quad (4)$$

where the variances under \mathcal{H}_0 and \mathcal{H}_1 can be expressed as

$$\delta_i^k = \begin{cases} |\mathbf{v}_k^H \mathbf{h}_0|^2 \sigma_s^2 + \sigma_w^2 \|\mathbf{v}_k\|^2, & i = 0 \\ |\mathbf{v}_k^H \mathbf{h}_1^k|^2 \sigma_s^2 + \sigma_w^2 \|\mathbf{v}_k\|^2, & i = 1. \end{cases} \quad (5)$$

Then, the received signals \mathbf{y}_k in one time interval obey the following distributions

$$\begin{cases} \mathcal{H}_0 : \mathbf{y}_k \sim \mathcal{CN}(\mathbf{0}, \mathbf{C}_0^k), & \mathbf{c}_k = \mathbf{0}, \\ \mathcal{H}_1 : \mathbf{y}_k \sim \mathcal{CN}(\mathbf{0}, \mathbf{C}_1^k), & \mathbf{c}_k = \mathbf{1}, \end{cases} \quad (6)$$

where the covariance matrices under \mathcal{H}_0 and \mathcal{H}_1 can be expressed as $\mathbf{C}_i^k = \delta_i^k \mathbf{I}_N$, $i \in \{0, 1\}$. \mathbf{c}_k denote the k -th tag's symbols in one time interval.

Correspondingly, the probability density function (PDF) under \mathcal{H}_0 and \mathcal{H}_1 can be expressed as

$$\begin{aligned} p_{\mathbf{y}_k | \mathcal{H}_i} &= \frac{1}{\pi^N \det(\mathbf{C}_i^k)} \exp(-\mathbf{y}_k^H (\mathbf{C}_i^k)^{-1} \mathbf{y}_k) \\ &= \frac{1}{\pi^N (\delta_i^k)^N} \exp\left(-\frac{\mathbf{y}_k^H \mathbf{y}_k}{\delta_i^k}\right), \quad i \in \{0, 1\}, \end{aligned} \quad (7)$$

The KLD can be used to approximate the likelihood ratio decision [28], [29]. Specifically, given two PDF $\mathbf{p}(x)$ and $\mathbf{q}(x)$, the KLD can be expressed as $D_{\text{KL}}(\mathbf{p}||\mathbf{q}) = \int \mathbf{p}(x) \ln\left(\frac{\mathbf{p}(x)}{\mathbf{q}(x)}\right) dx$. Thus, the KLD of the corresponding PDF of the reader under different hypotheses is

$$\begin{aligned} D_{\text{KL}}^k(p_{\mathbf{y}_k | \mathcal{H}_0} || p_{\mathbf{y}_k | \mathcal{H}_1}) &= \ln \frac{\det \mathbf{C}_1^k}{\det \mathbf{C}_0^k} + \text{Tr}((\mathbf{C}_1^k)^{-1} \mathbf{C}_0^k) - N \\ &= N \ln \frac{\delta_1^k}{\delta_0^k} + N \frac{\delta_0^k}{\delta_1^k} - N. \end{aligned} \quad (8)$$

Similarly, when the DL is available (i.e., $\bar{\mathbf{h}}_0 = \mathbf{0}$, and $\bar{\mathbf{h}}_1^k = \mathbf{h}_{\text{STR}}^k$), the received signals $\bar{\mathbf{y}}_k$ in one time interval obey the following distributions

$$\begin{cases} \mathcal{H}_0 : \bar{\mathbf{y}}_k \sim \mathcal{CN}(\mathbf{0}, \bar{\mathbf{C}}_0^k), \mathbf{c}_k = \mathbf{0}, \\ \mathcal{H}_1 : \bar{\mathbf{y}}_k \sim \mathcal{CN}(\mathbf{0}, \bar{\mathbf{C}}_1^k), \mathbf{c}_k = \mathbf{1}, \end{cases} \quad (9)$$

where $\bar{\mathbf{C}}_i^k = \delta_i^k \mathbf{I}_N$ are the covariance matrices, and

$$\delta_i^k = \begin{cases} |\mathbf{v}_k^H \bar{\mathbf{h}}_0|^2 \sigma_s^2 + \sigma_w^2 \|\mathbf{v}_k\|^2, i = 0, \\ |\mathbf{v}_k^H \bar{\mathbf{h}}_1^k|^2 \sigma_s^2 + \sigma_w^2 \|\mathbf{v}_k\|^2, i = 1. \end{cases} \quad (10)$$

Thus, the KLD of the corresponding PDF of the reader under different hypotheses without the DL can be expressed as

$$\begin{aligned} D_{\text{KL}}^k(p_{\bar{\mathbf{y}}_k|H_0} || p_{\bar{\mathbf{y}}_k|H_1}) \\ &= \ln \frac{\det \bar{\mathbf{C}}_1^k}{\det \bar{\mathbf{C}}_0^k} + \text{Tr}((\bar{\mathbf{C}}_1^k)^{-1} \bar{\mathbf{C}}_0^k) - N \\ &= N \ln \frac{\delta_1^k}{\delta_0^k} + N \frac{\delta_0^k}{\delta_1^k} - N. \end{aligned} \quad (11)$$

III. PROBLEM FORMULATION AND ALGORITHM DESIGN

In this section, an optimization problem is formulated to exploit the CI via beamforming design and tag selection with the objective of maximizing the received signal power. Two greedy-based algorithms are proposed for problem solving. Besides, a closed-form expression for the upper bound on the angle between the DL and the BL is revealed to shed light on the CI for the single-antenna reader.

A. Problem Formulation

In order to enhanced the received signal strength and guarantee the bit error rate (BER) of backscattered signal detection, an optimization problem for maximizing the received signal power at the reader is formulated subject to the KLD constraints, which is given by

$$\begin{aligned} \max_{\mathbf{v}_k, \beta_k} \quad & \sum_{k=1}^K \beta_k |\mathbf{v}_k^H \mathbf{h}_1^k|^2 \sigma_s^2, \\ \text{s.t.} \quad & \mathbf{C}_1 : \sum_{k=1}^K \beta_k = 1, \beta_k \in \{0, 1\}, \\ & \mathbf{C}_2 : \|\mathbf{v}_k\|^2 = 1, \forall k \\ & \mathbf{C}_3 : \Delta D_{\text{KL}}^k \geq 0, \forall k \\ & \mathbf{C}_4 : D_{\text{KL}}^k(p_{\bar{\mathbf{y}}_k|H_0} || p_{\bar{\mathbf{y}}_k|H_1}) \geq D_{\text{KL}}^{\text{th}}, \forall k \end{aligned} \quad (12)$$

where $D_{\text{KL}}^{\text{th}}$ denotes the minimum required KLD for backscattered signal detection¹. ΔD_{KL}^k is the gap between two KLDs with and without the DL for the k -th tag, which is expressed as

$$\begin{aligned} \Delta D_{\text{KL}}^k &= D_{\text{KL}}^k(p_{\mathbf{y}_k|H_0} || p_{\mathbf{y}_k|H_1}) - D_{\text{KL}}^k(p_{\bar{\mathbf{y}}_k|H_0} || p_{\bar{\mathbf{y}}_k|H_1}) \\ &= N \left[\ln \frac{\delta_1^k}{\delta_0^k} + \frac{\delta_0^k}{\delta_1^k} - \left(\ln \frac{\bar{\delta}_1^k}{\bar{\delta}_0^k} + \frac{\bar{\delta}_0^k}{\bar{\delta}_1^k} \right) \right]. \end{aligned} \quad (13)$$

¹It is noted that $D_{\text{KL}}^{\text{th}}$ is related to the detection error probability (see, such as [30]–[32]) for signal detection.

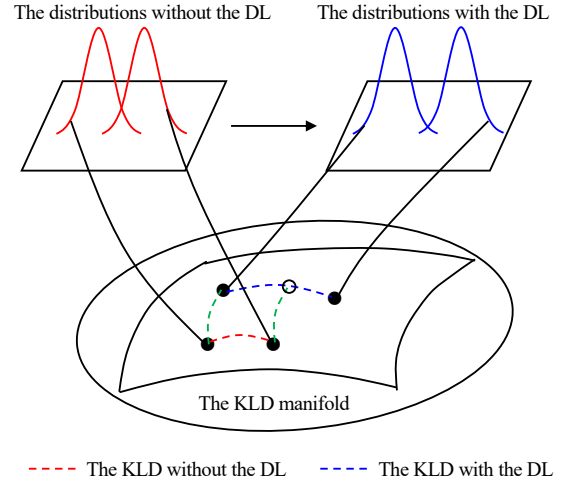


Fig. 2. A schematic manifold for the KLD.

Remark 1: It is well known that KLD can measure the distance between two random distributions. When two random distributions are the same, their KLD is almost zero. Otherwise, the greater the distance between two random distributions, the larger their KLD, which means the lower probability of error and the higher accuracy of signal detection can be obtained. As shown in Fig. 2, the KLDs under the different distributions with and without the DL are labelled on the KLD manifold. Our purpose is to explore whether it is possible to create a larger KLD by using the DL compared to that without the DL. By doing so, we can effectively improve the detection accuracy of the backscattered signal and reduce the BER of the BackCom system.

B. Problem Transformation and Algorithm Design

As can be seen, problem (12) is hard to solve directly due to the mixed-integer objective and the non-smooth constraints. To make it more treatable, assuming the k -th tag has been selected, the sub-problem for beamforming design can be transformed as

$$\begin{aligned} \max_{\mathbf{v}_k} \quad & |\mathbf{v}_k^H \mathbf{h}_1^k|^2 \sigma_s^2 \\ \text{s.t.} \quad & \mathbf{C}_2 - \mathbf{C}_4. \end{aligned} \quad (14)$$

However, it is still difficult to solve problem (14) due to the tight coupled relationship in \mathbf{C}_3 and \mathbf{C}_4 . To deal with it, we propose Theorem 1.

Theorem 1: \mathbf{C}_3 and \mathbf{C}_4 can be transformed into the equivalent forms, i.e.,

$$\bar{\mathbf{C}}_3 : |\mathbf{v}_k^H \mathbf{h}_1^k|^2 - |\mathbf{v}_k^H \mathbf{h}_0|^2 - |\mathbf{v}_k^H \bar{\mathbf{h}}_1^k|^2 \geq \gamma |\mathbf{v}_k^H \mathbf{h}_0|^2 |\mathbf{v}_k^H \bar{\mathbf{h}}_1^k|^2, \quad (15)$$

and

$$\bar{\mathbf{C}}_4 : \gamma |\mathbf{v}_k^H \bar{\mathbf{h}}_1^k|^2 \geq \exp(W_0(-\exp(-f_{\min}))) + f_{\min} - 1, \quad (16)$$

where $\gamma = \frac{\sigma_s^2}{\sigma_w^2}$ denotes the input signal-to-noise ratio (SNR) and $f_{\min} = \frac{D_{\text{KL}}^{\text{th}}}{N} + 1$.

Proof: Please see Appendix A.

Based on Theorem 1, problem (14) can be transformed into the following problem, i.e.,

$$\begin{aligned} & \max_{\mathbf{v}_k} |\mathbf{v}_k^H \mathbf{h}_1^k|^2 \sigma_s^2 \\ & \text{s.t. } \bar{C}_2, \bar{C}_3, \bar{C}_4. \end{aligned} \quad (17)$$

It is noted that

$$\mathbf{v}_k^H \mathbf{X} \mathbf{v}_k = \text{Tr}(\mathbf{v}_k^H \mathbf{X} \mathbf{v}_k) = \text{Tr}(\mathbf{X} \mathbf{v}_k \mathbf{v}_k^H). \quad (18)$$

Then, by introducing a new variable $\mathbf{W}_k = \mathbf{v}_k \mathbf{v}_k^H$, \bar{C}_3 and \bar{C}_4 can be transformed, respectively, as

$$\begin{aligned} & \text{Tr}(\mathbf{A}_k \mathbf{W}_k) - \text{Tr}(\mathbf{B}_0 \mathbf{W}_k) - \text{Tr}(\mathbf{C}_k \mathbf{W}_k) \\ & \geq \gamma \text{Tr}(\mathbf{B}_0 \mathbf{W}_k) \text{Tr}(\mathbf{C}_k \mathbf{W}_k), \end{aligned} \quad (19)$$

and

$$\gamma \text{Tr}(\mathbf{C}_k \mathbf{W}_k) \geq \exp(W_0(-\exp(-f_{\min})) + f_{\min}) - 1, \quad (20)$$

where $\mathbf{A}_k = \mathbf{h}_1^k (\mathbf{h}_1^k)^H$, $\mathbf{B}_0 = \mathbf{h}_0 \mathbf{h}_0^H$, and $\mathbf{C}_k = \bar{\mathbf{h}}_1^k (\bar{\mathbf{h}}_1^k)^H$.

Thus, problem (17) can be finally expressed as

$$\begin{aligned} & \max_{\mathbf{W}_k} \text{Tr}(\mathbf{A}_k \mathbf{W}_k) \sigma_s^2 \\ & \text{s.t. } \bar{C}_2 : \text{Tr}(\mathbf{W}_k) = 1, \\ & \hat{C}_3 : \text{Tr}(\mathbf{A}_k \mathbf{W}_k) - \text{Tr}(\mathbf{B}_0 \mathbf{W}_k) - \text{Tr}(\mathbf{C}_k \mathbf{W}_k) \\ & \quad \geq \gamma \text{Tr}(\mathbf{B}_0 \mathbf{W}_k) \text{Tr}(\mathbf{C}_k \mathbf{W}_k), \\ & \hat{C}_4 : \gamma \text{Tr}(\mathbf{C}_k \mathbf{W}_k) \geq \exp(W_0(-\exp(-f_{\min})) + f_{\min}) - 1, \\ & \bar{C}_5 : \text{Rank}(\mathbf{W}_k) = 1. \end{aligned} \quad (21)$$

However, problem (21) is still a non-convex problem caused by the non-convexity in \hat{C}_3 . In general, it is difficult or even intractable to obtain the global optimal solution to such a non-convex problem. To make it more treatable, we introduce two slack variables t_k and l_k such that $\text{Tr}(\mathbf{B}_0 \mathbf{W}_k) \leq t_k$ and $\text{Tr}(\mathbf{C}_k \mathbf{W}_k) \leq l_k$, respectively, and problem (21) can be transformed as

$$\begin{aligned} & \max_{\mathbf{W}_k, t_k, l_k} \text{Tr}(\mathbf{A}_k \mathbf{W}_k) \sigma_s^2 \\ & \text{s.t. } \bar{C}_2, \bar{C}_5, \\ & \check{C}_3 : \text{Tr}(\mathbf{A}_k \mathbf{W}_k) - t_k - l_k \geq \gamma t_k l_k, \\ & \tilde{C}_4 : \gamma l_k \geq \exp(W_0(-\exp(-f_{\min})) + f_{\min}) - 1, \\ & C_6 : \text{Tr}(\mathbf{B}_0 \mathbf{W}_k) \leq t_k, \\ & C_7 : \text{Tr}(\mathbf{C}_k \mathbf{W}_k) \leq l_k, \end{aligned} \quad (22)$$

Assuming that t_k and l_k are given, we have

$$\begin{aligned} & \max_{\mathbf{W}_k} \text{Tr}(\mathbf{A}_k \mathbf{W}_k) \sigma_s^2 \\ & \text{s.t. } \bar{C}_2 - C_7. \end{aligned} \quad (23)$$

By removing the rank constraint, problem (23) is relaxed into an SDP problem, namely

$$\begin{aligned} & \max_{\mathbf{W}_k} \text{Tr}(\mathbf{A}_k \mathbf{W}_k) \sigma_s^2 \\ & \text{s.t. } \bar{C}_2 - \tilde{C}_4, C_6, C_7. \end{aligned} \quad (24)$$

Note that after the SDP relaxation of problem (23), problem (24) is convex and can be solved efficiently by existing commercial solvers [33]. In general, the optimal objective

Algorithm 1 The VRBA for Beamforming Design

Input: $K, M, N, \alpha_k, h_{\text{ST}}^k, \mathbf{h}_{\text{SR}}, \mathbf{h}_{\text{TR}}^k, \sigma_w^2, \sigma_s^2$.

Set: Choose large T and L . Define $\Delta t_k = (t_k^{\text{ub}} - t_k^{\text{lb}})/T$ and $\Delta l_k = (l_k^{\text{ub}} - l_k^{\text{lb}})/L$.

Initialize: $S^{\text{One}} = 0$.

Output: \mathbf{v}_k .

```

1: for  $i = 0 : T$ 
2:   Set  $t_k = i \Delta t_k + t_k^{\text{lb}}$ .
3:   for  $j = 0 : L$ 
4:     Set  $l_k = j \Delta l_k + l_k^{\text{lb}}$ .
5:     Solve problem (24), obtain  $\mathbf{W}_k^*$ 
6:     if  $\text{Tr}(\mathbf{A}_k \mathbf{W}_k^*) \sigma_s^2 \geq S^{\text{One}}$ 
7:       Update  $S^{\text{One}} = \text{Tr}(\mathbf{A}_k \mathbf{W}_k^*) \sigma_s^2$ 
8:     end if
9:   end for
10: end for
```

value of the SDP relaxation (24) is a lower bound of the optimal value of the original problem (23) [34]. If the optimal solution of the SDP relaxation, \mathbf{W}_k^* is rank-one, the optimal solution of problem (17), \mathbf{v}_k^* can be recovered from \mathbf{W}_k^* by solving $\mathbf{W}_k^* = \mathbf{v}_k^* (\mathbf{v}_k^*)^H$. However, if the rank of \mathbf{W}_k^* is larger than one, the Gaussian randomization method can be applied [35]. Besides, t_k and l_k can be determined by the two-dimensional (2-D) search. Specifically, the upper and lower bounds of t_k can be chosen as [36], respectively,

$$\begin{cases} t_k^{\text{ub}} = \max_{\mathbf{W}_k} \text{Tr}(\mathbf{B}_0 \mathbf{W}_k) = \lambda_k^{\max}(\mathbf{B}_0), \\ t_k^{\text{lb}} = \min_{\mathbf{W}_k} \text{Tr}(\mathbf{B}_0 \mathbf{W}_k) = \lambda_k^{\min}(\mathbf{B}_0). \end{cases} \quad (25)$$

Similarly, the upper and lower bounds of l_k can be chosen as, respectively,

$$\begin{cases} l_k^{\text{ub}} = \max_{\mathbf{W}_k} \text{Tr}(\mathbf{C}_k \mathbf{W}_k) = \lambda_k^{\max}(\mathbf{C}_k), \\ l_k^{\text{lb}} = \min_{\mathbf{W}_k} \text{Tr}(\mathbf{C}_k \mathbf{W}_k) = \lambda_k^{\min}(\mathbf{C}_k). \end{cases} \quad (26)$$

The detail of this algorithm is shown in **Algorithm 1**. Here, the computational complexity of the proposed variable relaxation-based algorithm (VRBA) is evaluated. Before solving problem (24), it needs $\mathcal{O}(TL)$ to determine the variables t_k and l_k . Letting ω_1 denotes the iterative accuracy, the computational complexity for solving problem (24) via CVX in each iteration $\mathcal{O}(M^7 \ln(\frac{1}{\omega_1}))$. Therefore, the total computation complexity is $\mathcal{O}(TLM^7 \ln(\frac{1}{\omega_1}))$.

C. Low Complexity-Based Algorithm (LCBA)

In the **Algorithm 1**, the 2-D search over (l_k, t_k) has a high computational complexity. In order to reduce the computational complexity of **Algorithm 1**, in this subsection, we propose and investigate another solution for problem (21). By only introducing a slack variable t_k such that $\text{Tr}(\mathbf{B}_0 \mathbf{W}_k) \leq t_k$, problem (21) can be transformed into the following problem,

Algorithm 2 The LCBA for Beamforming Design

Input: $K, M, N, \alpha_k, h_{\text{ST}}^k, \mathbf{h}_{\text{SR}}, \mathbf{h}_{\text{TR}}^k, \sigma_w^2, \sigma_s^2$.
Set: Choose a large T . Define $\Delta t_k = (t_k^{\text{ub}} - t_k^{\text{lb}})/T$.
Initialize: $S^{\text{Two}} = 0$.
Output: \mathbf{v}_k .
1: **for** $i = 0 : T$
2: Set $t_k = i\Delta t_k + t_k^{\text{lb}}$.
3: Solve problem (29), obtain \mathbf{W}_k^*
4: **if** $\text{Tr}(\mathbf{A}_k \mathbf{W}_k^*) \sigma_s^2 \geq S^{\text{Two}}$
5: Update $S^{\text{Two}} = \text{Tr}(\mathbf{A}_k \mathbf{W}_k^*) \sigma_s^2$
6: **end if**
7: **end for**

i.e.,

$$\begin{aligned} & \max_{\mathbf{W}_k, t_k} \text{Tr}(\mathbf{A}_k \mathbf{W}_k) \sigma_s^2 \\ & \text{s.t. } \bar{C}_2, \hat{C}_4, C_5, \\ & \quad \bar{C}_3 : \text{Tr}(\mathbf{A}_k \mathbf{W}_k) - t_k - \text{Tr}(\mathbf{C}_k \mathbf{W}_k) \geq \gamma t_k \text{Tr}(\mathbf{C}_k \mathbf{W}_k), \\ & \quad C_6 : \text{Tr}(\mathbf{B}_0 \mathbf{W}_k) \leq t_k. \end{aligned} \quad (27)$$

It is noted that \bar{C}_3 is handled more efficiently comparing to the VRBA and thus avoid the high complexity caused by the 2-D search method. Assuming that t_k is determined as (25), we have

$$\begin{aligned} & \max_{\mathbf{W}_k} \text{Tr}(\mathbf{A}_k \mathbf{W}_k) \sigma_s^2 \\ & \text{s.t. } \bar{C}_2 - C_6. \end{aligned} \quad (28)$$

Consider the rank-one relaxation of (28) as follows

$$\begin{aligned} & \max_{\mathbf{W}_k} \text{Tr}(\mathbf{A}_k \mathbf{W}_k) \sigma_s^2 \\ & \text{s.t. } \bar{C}_2 - \hat{C}_4, C_6. \end{aligned} \quad (29)$$

Problem (29) can be solved via CVX [33]. The detail of the proposed low complexity-based algorithm (LCBA) is shown in **Algorithm 2**. Here, the computational complexity of this algorithm is evaluated. Before solving problem (29), it needs $\mathcal{O}(T)$ to determine the variable t_k . Letting ω_2 denotes the iterative accuracy, the computational complexity for solving problem (24) via CVX in each iteration $\mathcal{O}(M^7 \ln(\frac{1}{\omega_2}))$. Therefore, the total computation complexity is $\mathcal{O}(TM^7 \ln(\frac{1}{\omega_2}))$. It can be seen that, the complexity of the LCBA is much smaller than that of the VRBA and is almost only $\frac{1}{L}$ to the VRBA.

Besides, the remaining sub-problem for tag selection is a 0/1 nonlinear optimization problem, which is NP-complete. To deal with it, a greedy algorithm, a mechanism to approximate global optimal solution by searching a series of locally optimal alternatives which is effective but with a low complexity, is applied [37]. The detail of the greedy algorithm is shown in **Algorithm 3**. Furthermore, when the beamforming design is determined, it costs $\mathcal{O}(K)$ for tag selection in **Algorithm 3**.

D. A Special Case: A Single-Antenna Reader

In previous subsections, we consider a multiple-antenna reader, where the CI can be guaranteed by the reader beamforming design. In this subsection, in order to gain more

Algorithm 3 The Greedy algorithm for Tag Selection

Input: $K, M, N, \alpha_k, h_{\text{ST}}^k, \mathbf{h}_{\text{SR}}, \mathbf{h}_{\text{TR}}^k, \sigma_w^2, \sigma_s^2$.
Initialize: $S^{\text{GA}} = 0$.
Output: β_k .
1: **for** $k = 1 : K$
2: Solve problem (21), obtain \mathbf{v}_k^* using the VRBA in **Algorithm 1** or the LCBA in **Algorithm 2**.
3: Update $S_k^* = |(\mathbf{v}_k^*)^H \mathbf{h}_1|^2 \sigma_s^2$.
4: **if** $S_k^* > S^{\text{GA}}$
5: Update $S^{\text{GA}} = S_k^*, \beta_k^* = 1$.
6: **else if**
7: Update $\beta_k^* = 0$.
8: **end if**
9: **end for**

insight into the CI, we consider the single-antenna reader to facilitate our analysis on the CI. The received signal of the reader from the PS and the k -th tag can be expressed as

$$y_k(n) = h_{\text{SR}} s(n) + \sqrt{\alpha_k} \beta_k h_{\text{STR}}^k s(n) c_k(n) + w(n), \quad (30)$$

where $h_{\text{SR}} \in \mathbb{C}^{1 \times 1}$ and $h_{\text{STR}}^k = h_{\text{ST}}^k h_{\text{TR}}^k$ denote the channel coefficients of the DL and the BL, respectively. $h_{\text{ST}}^k \in \mathbb{C}^{1 \times 1}$ and $h_{\text{TR}}^k \in \mathbb{C}^{1 \times 1}$ are the channel coefficients of the forward link and backward link for the k -th tag. $w(n)$ is the noise at the reader with zero mean and variance σ_w^2 .

Similar to previous analysis on the KLD, to make the DLI constructive, the following KLD constraint for the k -th tag need to be satisfied

$$\Delta D_{\text{KL}}^k = N \left[\left(\ln \frac{\delta_1^k}{\bar{\delta}_0} + \frac{\delta_0}{\delta_1^k} \right) - \left(\ln \frac{\bar{\delta}_1^k}{\bar{\delta}_0} + \frac{\bar{\delta}_0}{\bar{\delta}_1^k} \right) \right] \geq 0. \quad (31)$$

where $\delta_0 = \sigma_s^2 |h_0|^2 + \sigma_w^2$, $\bar{\delta}_0 = \sigma_s^2 |\bar{h}_0|^2 + \sigma_w^2$, $\delta_1^k = \sigma_s^2 |h_1^k|^2 + \sigma_w^2$, $\bar{\delta}_1^k = \sigma_s^2 |\bar{h}_1^k|^2 + \sigma_w^2$, $h_0 = h_{\text{SR}}$, $\bar{h}_0 = 0$, $h_1^k = h_{\text{SR}} + h_{\text{STR}}^k$, and $\bar{h}_1^k = h_{\text{STR}}^k$.

On the other hand, considering the minimum KLD requirement, we have

$$N \left(\ln \frac{\bar{\delta}_1^k}{\bar{\delta}_0} + \frac{\bar{\delta}_0}{\bar{\delta}_1^k} - 1 \right) \geq D_{\text{KL}}^{\text{th}}. \quad (32)$$

To reveal the CI region, theorem 2 is proposed.

Theorem 2: The resulting DLI is constructive when the input SNR (γ) is satisfied, i.e.,

$$\begin{aligned} & \frac{\exp(W_0(-\exp(-f_{\text{min}})) + f_{\text{min}}) - 1}{|h_{\text{STR}}^k|^2} \leq \\ & \gamma \leq \frac{(h_{\text{SR}})^H h_{\text{STR}}^k + h_{\text{SR}} (h_{\text{STR}}^k)^H}{|h_{\text{SR}}|^2 |h_{\text{STR}}^k|^2}. \end{aligned} \quad (33)$$

Proof: Please see Appendix B.

Remark 2: From (33), it can be seen that the actual CI region for γ is obtained. That is to say, the introduced DLI is constructive for BackCom systems when γ lies within this region. Besides, as f_{min} become larger, the demand for γ will become more strict accordingly, and the system may not be able to achieve the desired performance with a small γ . On the other hand, when the DL (h_{SR}) becomes large, it will degrade

the upper bound of γ , which is obvious for the system not to achieve the CI.

To further show the relationship between the BL and the DL, we give theorem 3.

Theorem 3: Letting $\theta_k \triangleq \angle \langle h_{SR}, h_{STR}^k \rangle$ denote the angle between the DL and the BL, the resulting DLI is constructive when θ_k satisfies the following condition, i.e.,

$$0 \leq \theta_k \leq \min \left\{ \frac{\pi}{2}, \arccos \frac{1}{2} \gamma |h_{SR}| |h_{STR}^k| \right\}, \quad (34)$$

where $\gamma \geq \frac{\exp(W_0(-\exp(-f_{\min})) + f_{\min}) - 1}{|h_{STR}^k|^2}$.

Proof: Please see Appendix C.

Remark 3: It can be seen that from (34), the CI angle can be expressed as $\min \{ \frac{\pi}{2}, \arccos \frac{1}{2} \gamma |h_{SR}| |h_{STR}^k| \}$. Specifically, $\arccos \frac{1}{2} \gamma |h_{SR}| |h_{STR}^k|$ is gradually closed to $\frac{\pi}{2}$ with the decreasing γ , $|h_{STR}^k|$, and/or $|h_{SR}|$. By doing so, the CI angle can be enlarged, however, the received signal power is reduced accordingly, which is a contradiction to our original intention. On the other hand, in order to guarantee the minimum KLD requirement, the maximum angle for signal detection needs to satisfy $\theta_k^{\max} = \arccos \frac{1}{2} \gamma^{\min} |h_{SR}| |h_{STR}^k|$, where $\gamma^{\min} = \frac{\exp(W_0(-\exp(-f_{\min})) + f_{\min}) - 1}{|h_{STR}^k|^2}$. Specifically, θ_k^{\max} is decreased with the decreasing $|h_{STR}^k|$ and the increasing $|h_{SR}|$ and f_{\min} . That is to say, it is not conducive to the establishment of CI if the DL is too strong and/or the minimum KLD requirement is too large. The simulations below also verify what we have analyzed.

IV. SIMULATION RESULTS

In this section, we present the simulation results of our proposed algorithms for BackCom networks. We assume that there are one PS, one reader with 4 antennas (i.e., $M = 4$), and 5 tags (i.e., $K = 5$) in the proposed system. The distances between the PS and tags, the PS and the reader, as well as the reader to tags are both within 3 meters. We consider the distance-dependent pathloss as large scale fading, where the path-loss exponent is 3, and Rician fading with the Rician factor is 2.8 dB [18]. w_k is set to follow $\mathcal{CN}(0, 0.03)$ [38]. Other parameters include $N = 400$, $\alpha_k = 0.8$, $D_{KL}^{\text{th}} = 24$, $T = 10^3$, and $L = 10^3$. Finally, the simulation results are evaluated based on the CVX package [39].

A. CI Region with SIMO

In this subsection, we begin by investigating the region of the CI for SIMO-based BackComs. For algorithm comparison, we define three benchmark algorithms, such as

- **The algorithm without DL**

In this algorithm, we assume that there is no DL, that is to say, only the BL can be received by the reader. However, the requirement of the minimum KLD needs to be satisfied.

- **The algorithm without KLD**

In this algorithm, we assume that there is no requirement of the KLD, that is to say, although, the DL is available, we do not consider whether the resulting DLI is constructive or destructive.

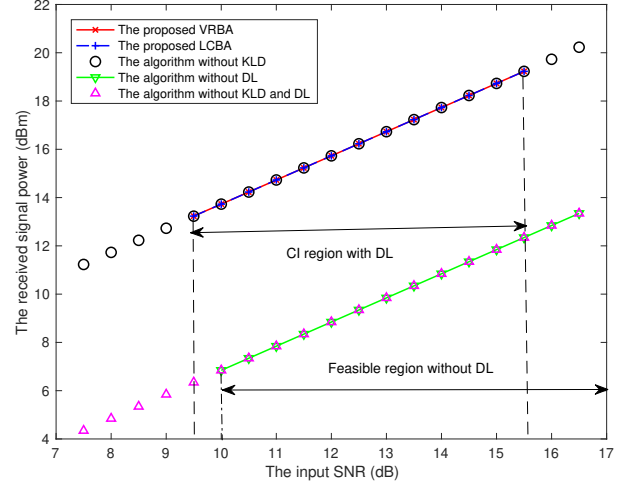


Fig. 3. The received signal power versus the input SNR (γ).

- **The algorithm without DL and KLD**

In this algorithm, we assume that there is no DL, meanwhile the requirement of the minimum KLD is not taken into consideration.

The purpose is to evaluate the performance and effectiveness of the proposed algorithms under different aspects by comparing them with benchmark algorithms. On the one hand, by comparing with algorithms without the KLD, we can measure the impact of introducing CI on the system performance, due to the fact that the algorithms without the KLD can achieve a performance upper bound. On the other hand, by comparing with the algorithms without the DL, we can evaluate the effectiveness of the proposed algorithms in enhancing the received signal power. In the following, we compare the proposed algorithms with these benchmark algorithms with respect to the input SNR, the number of receive antennas, and the channel gain of the DL, respectively, to demonstrate the performance and implications of the proposed algorithms.

Fig. 3 shows the received signal power versus the input SNR (γ). As we expect, the received signal power increased by increasing γ for all algorithms. However, it should be noted that when KLD constraints are not considered, all power domains are feasible; when KLD constraints are considered, the feasible domain, i.e., the CI region, is compressed into a limited region. This behavior is due to the fact that when γ is relatively small, the minimum KLD requirement cannot be satisfied, which means that the BER for signal detection will not be guaranteed. On the other hand, when γ is relatively large, the KLD with the DL is no longer large than that without the DL, which implies that the resulting DLI is destructive. Besides, in the CI region, the received signal power for the proposed VRBA/LCBA is larger than that for the algorithms without the DL. This indicates the received signal strength is increased, which contributes to improving the accuracy of weak signal detection and reducing the BER.

Fig. 4 shows the received signal power versus the number of receive antennas (M) with a small input SNR (i.e., $\gamma = 13$

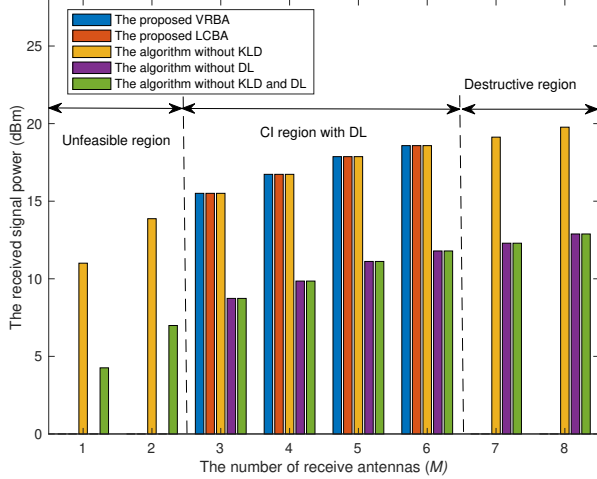


Fig. 4. The received signal power versus the number of antennas (M).

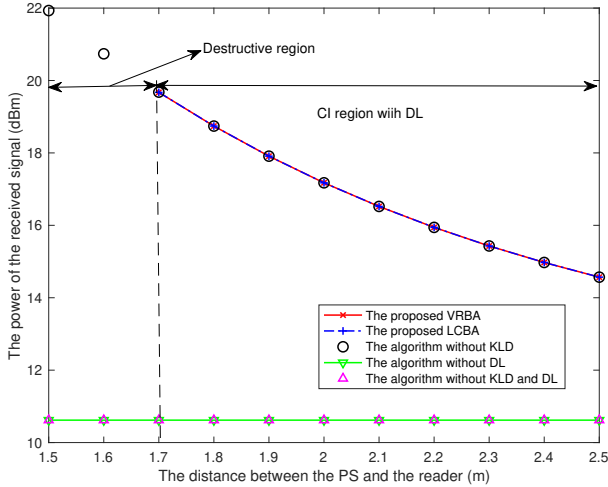


Fig. 5. The received signal power versus the distance between the PS and the reader.

dB). It is seen that as M increases, the received signal power for all algorithms also increases gradually, which is attributed to the improvement in channel gain due to the increase in M . Besides, the proposed algorithms are not feasible when M is too small and too large. This is because when M is small, the signal detection requirement for the algorithms with KLD constraints cannot be satisfied. On the other hand, when M is relatively large, the signal from the DL is too strong to keep the DLI constructive due to the better channel gain of the DL. Moreover, the received signal power for the proposed VRBA/LCBA is the highest in the CI region. This reveals that when the input SNR is small, the received signal power can be enhanced by increasing the number of receive antennas appropriately. Besides, it is worth noting that although the proposed algorithms achieve the same effect from Fig. 3 and Fig. 4, the resulting complexity is far different, which has been analyzed in Subsection C of Section III.

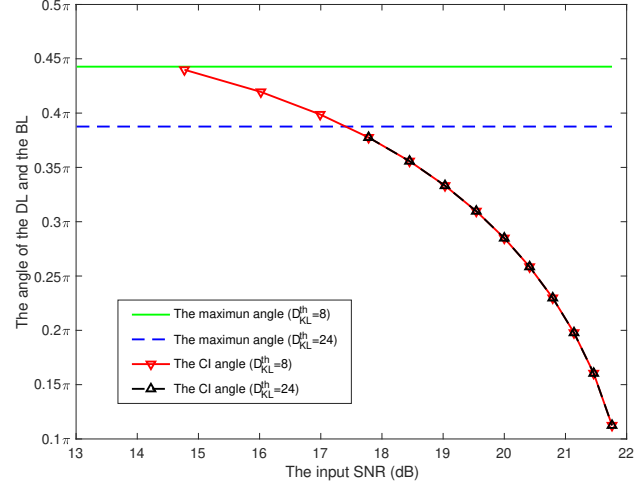


Fig. 6. The angle between the DL and the BL versus the input SNR (γ).

Fig. 5 shows the received signal power versus the distance between the PS and the reader (i.e., the DL distance). It can be seen that, with the increase of the DL distance, the received signal power for the algorithms with the DL gradually decreases and that for algorithms without the DL keeps unchanged. The reason is that the increase of the DL distance reduces its channel gain. Besides, the received signal power for the proposed VRBA/LCBA is always higher than that for the algorithms without the DL. However, when the DL distance is less than 1.7m, the proposed algorithms collapse. It can be inspired that, in order to better enhance the benefits of the DLI, the DL distance can be appropriately reduced to increase the received signal strength.

B. CI Angle for SISO

In this subsection, we numerically evaluate the angle between the DL and the BL with the CI constraint, as shown in Fig. 6, 7, and 8, respectively, for single input single output (SISO)-based BackComs.

To be specific, Fig. 6 shows the angle between the DL and the BL versus γ . As can be seen, the CI angle between the DL and the BL decreases as the γ becomes larger and is always smaller than the maximum angle. The reason is that when only the minimum KLD constraint needs to be satisfied, the requirement for the DL is low, and the channel angle is relatively large, which is close to orthogonal. On the other hand, in order to enhance the received signal power, the demand for the DL has to increase, so the channel angle is correspondingly reduced. However, it does not mean that the larger the γ , the better the performance. As shown in the figure, when γ is too large, the channel angle no longer exists. This is because the over-saturated input SNR also brings so much DLI that the CI region cannot be kept. Besides, under different D_{KL}^{th} , the upper bound of the CI angle is also different, since it needs enough power to satisfy the corresponding requirement for signal detection.

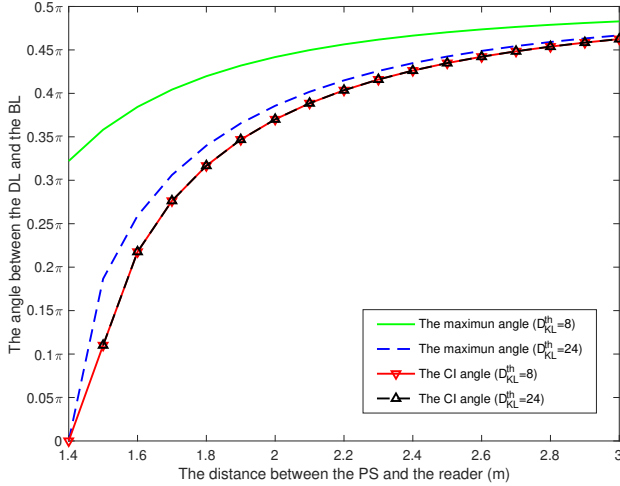


Fig. 7. The angle between the DL and the BL versus the distance between the PS and the reader.

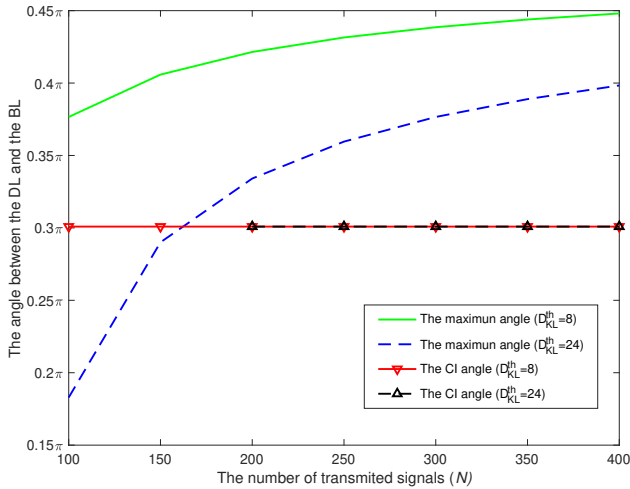


Fig. 8. The angle between the DL and the BL versus the number of the transmitted signals (N).

Fig. 7 shows the angle between the DL and the BL versus the DL distance. From the figure, both the maximum angle and the CI angle are increasing with the increasing DL distance, and the gap between them becomes smaller. The reason is that when the DL distance becomes larger, the channel gain of the DL decreases, which directly leads to a decrease in the received signal strength. In particular, when the DL distance is relatively large, the channel gain of the DL will be pretty small, even close to 0, and the system will be approximately transformed into the one without the DL. Therefore, in order to improve the received signal strength, it is necessary to reduce the DL distance. Besides, the CI angle with a large KLD is not available when the DL distance is smaller than 1.5m. The reason is that it is too hard for the DLI to keep constructive under such a short DL distance due to the overpowering channel gain of the DL.

Fig. 8 shows the angle between the DL and the BL versus the number of the transmitted signals (N). From the figure, as N increases, the maximum angle increases, and the CI angle keeps unchanged. This is because when the channel gains of the DL and the BL are known, the maximum angle is a monotonic increase with respect to N , while the CI angle is only affected by γ . Besides, the CI angle with a larger KLD (i.e., $D_{\text{KL}}^{\text{th}} = 24$) is not available when N is smaller than 200. The reason is that from (11), when N is small, the minimum KLD requirement for each transmitted signal gets large. Thus, once the input SNR is too small to satisfy the corresponding $D_{\text{KL}}^{\text{th}}$, the CI region of the DLI becomes unavailable. That is to say, appropriately increasing N is helpful to build the CI angle and expanding the CI region.

V. CONCLUSIONS

This paper investigates and analyzes the CI region for BackComs with multiple tags and a mult-antennas reader, where tag selection and receive beamforming are taken into account. Specifically, a novel KLD-oriented approach is proposed to build the CI region for the DLI, and an optimization problem for maximizing the received signal power is formulated. Then, we decompose the original problem, and then propose two algorithms to solve the sub-problem with beamforming design via a change of variables, and SDP method and a greedy algorithm to solve the sub-problem with tag selection. Furthermore, a closed-form expression for the angle between the DL and the BL is derived in the BackCom system with a single-antenna reader. Simulation results show that the performance for the proposed algorithms outperform benchmark algorithms in terms of the received signal power, and confirm the derived channel angle for the CI.

APPENDIX A

PROOF OF THEOREM 1

Defining $f(x) = \ln x + \frac{1}{x}$, where $x > 0$, the first-order derivative of $f(x)$ is

$$\frac{\partial f(x)}{\partial x} = \frac{1}{x} - \frac{1}{x^2} = \begin{cases} < 0, & 0 < x < 1, \\ = 0, & x = 1, \\ > 0, & x > 1, \end{cases} \quad (35)$$

Letting $x_1^k = \frac{\delta^k}{\delta_0^k}$ and $x_0^k = \frac{\bar{\delta}^k}{\delta_0^k}$, we have

$$\begin{cases} x_1^k = \frac{|\mathbf{v}_k^H \mathbf{h}_1^k|^2 \sigma_s^2 + \sigma_w^2}{|\mathbf{v}_k^H \mathbf{h}_0|^2 \sigma_s^2 + \sigma_w^2} \\ = \frac{(|\mathbf{v}_k^H \mathbf{h}_1^k|^2 - |\mathbf{v}_k^H \mathbf{h}_0|^2) \sigma_s^2}{|\mathbf{v}_k^H \mathbf{h}_0|^2 \sigma_s^2 + \sigma_w^2} + 1 \geq 1, \\ x_0^k = \frac{|\mathbf{v}_k^H \bar{\mathbf{h}}_1^k|^2 \sigma_s^2 + \sigma_w^2}{\sigma_w^2} = \frac{|\mathbf{v}_k^H \bar{\mathbf{h}}_1^k|^2 \sigma_s^2}{\sigma_w^2} + 1 \geq 1. \end{cases} \quad (36)$$

Thus, C_4 can be written as

$$f(x_0^k) = \ln x_0^k + \frac{1}{x_0^k} \geq f_{\min}, \quad (37)$$

where $f_{\min} = \frac{D_{\text{KL}}^{\text{th}}}{N} + 1$.

As shown in the Fig. 9, there are two potential solution regions for x_0^k satisfying (37). According to the limitation of

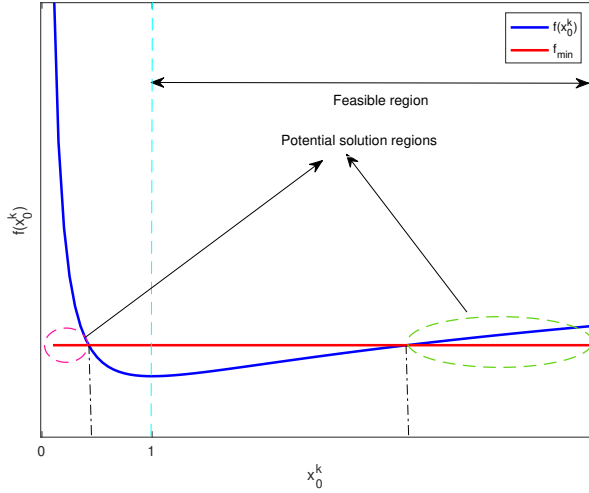


Fig. 9. The schematic diagram for $f(x_0^k)$.

the feasible region in (36), we can round off a solution region. However, it is still challenging to solve this inequality due to its non-convexity. To this end, taking (37) as an equivalent transformation, we have

$$(\ln x_0^k - f_{\min}) \exp(\ln x_0^k - f_{\min}) \geq -\exp(-f_{\min}). \quad (38)$$

Since $-\exp(-f_{\min}) \in [-\exp(-1), 0)$, based on Lambert W function [40], [41], we have

$$\begin{cases} \ln x_0^k - f_{\min} \leq W_{-1}(-\exp(-f_{\min})), 0 < x_0^k < 1, (\text{Neglect}) \\ \ln x_0^k - f_{\min} \geq W_0(-\exp(-f_{\min})), x_0^k \geq 1. \end{cases} \quad (39)$$

Thus, we can obtain the solutions of x_0^k , i.e.,

$$\begin{cases} x_0^k \leq \exp(W_{-1}(-\exp(-f_{\min})) + f_{\min}), 0 < x_0^k < 1, (\text{Neglect}) \\ x_0^k \geq \exp(W_0(-\exp(-f_{\min})) + f_{\min}), x_0^k \geq 1. \end{cases} \quad (40)$$

On the other hand, C_3 can be rewritten as

$$\ln x_1^k + \frac{1}{x_1^k} - (\ln x_0^k + \frac{1}{x_0^k}) \geq 0. \quad (41)$$

According to its monotonicity, we can equivalently convert $f(x_1^k) - f(x_0^k) \geq 0$ into $x_1^k \geq x_0^k$ and $x_1^k < x_0^k$ (which is neglected according to the feasible region). That is to say, C_3 can be transformed by the following form, i.e.,

$$\frac{|\mathbf{v}_k^H \mathbf{h}_1^k|^2 - |\mathbf{v}_k^H \mathbf{h}_0|^2}{|\mathbf{v}_k^H \mathbf{h}_0|^2 \sigma_s^2 + \sigma_w^2} \geq \frac{|\mathbf{v}_k^H \bar{\mathbf{h}}_1^k|^2}{\sigma_w^2}, \quad (42)$$

or equivalently

$$\frac{|\mathbf{v}_k^H \mathbf{h}_1^k|^2 - |\mathbf{v}_k^H \mathbf{h}_0|^2 - |\mathbf{v}_k^H \bar{\mathbf{h}}_1^k|^2}{|\mathbf{v}_k^H \mathbf{h}_0|^2 |\mathbf{v}_k^H \bar{\mathbf{h}}_1^k|^2} \geq \frac{\sigma_s^2}{\sigma_w^2}. \quad (43)$$

This completes the proof.

APPENDIX B

PROOF OF THEOREMS 2

According to (31), we can obtain

$$\ln \frac{\delta_1^k}{\delta_0} + \frac{\delta_0}{\delta_1^k} \geq \ln \frac{\bar{\delta}_1^k}{\bar{\delta}_0} + \frac{\bar{\delta}_0}{\bar{\delta}_1^k}. \quad (44)$$

Based on (41) and (42), (44) can be transformed into

$$\frac{\sigma_s^2 |h_1^k|^2 + \sigma_w^2}{\sigma_s^2 |h_0|^2 + \sigma_w^2} \geq \frac{\sigma_s^2 |\bar{h}_1^k|^2 + \sigma_w^2}{\sigma_s^2 |\bar{h}_0|^2 + \sigma_w^2}, \quad (45)$$

or equivalently

$$\begin{aligned} & \frac{|h_{\text{SR}} + h_{\text{STR}}^k|^2 - |h_{\text{SR}}|^2}{\sigma_s^2 |h_{\text{SR}}|^2 + \sigma_w^2} \geq \frac{|h_{\text{STR}}^k|^2}{\sigma_w^2} \\ \Leftrightarrow & (|h_{\text{SR}} + h_{\text{STR}}^k|^2 - |h_{\text{SR}}|^2 - |h_{\text{STR}}^k|^2) \sigma_w^2 \\ & \geq \sigma_s^2 |h_{\text{SR}}|^2 |h_{\text{STR}}^k|^2 \\ \Leftrightarrow & \frac{(h_{\text{SR}})^H h_{\text{STR}}^k + h_{\text{SR}} (h_{\text{STR}}^k)^H}{|h_{\text{SR}}|^2 |h_{\text{STR}}^k|^2} \geq \gamma. \end{aligned} \quad (46)$$

Besides, according to (37)–(40), (32) can be transformed into

$$\gamma \geq \frac{\exp(W_0(-\exp(-f_{\min})) + f_{\min}) - 1}{|h_{\text{STR}}^k|^2}, \quad (47)$$

Thus, the CI region with respect to γ can be expressed as

$$\begin{aligned} & \frac{\exp(W_0(-\exp(-f_{\min})) + f_{\min}) - 1}{|h_{\text{STR}}^k|^2} \leq \\ \gamma \leq & \frac{(h_{\text{SR}})^H h_{\text{STR}}^k + h_{\text{SR}} (h_{\text{STR}}^k)^H}{|h_{\text{SR}}|^2 |h_{\text{STR}}^k|^2}. \end{aligned} \quad (48)$$

This completes the proof.

APPENDIX C

PROOF OF THEOREMS 3

According to the definition of vectorial angle, we have

$$\cos \langle h_{\text{SR}}, h_{\text{STR}}^k \rangle = \frac{|\langle h_{\text{SR}}, h_{\text{STR}}^k \rangle|}{|h_{\text{SR}}| |h_{\text{STR}}^k|} = \frac{(h_{\text{SR}})^H h_{\text{STR}}^k}{|h_{\text{SR}}| |h_{\text{STR}}^k|}. \quad (49)$$

Similarly, we can obtain

$$\cos \langle h_{\text{STR}}^k, h_{\text{SR}} \rangle = \frac{(h_{\text{STR}}^k)^H h_{\text{SR}}}{|h_{\text{SR}}| |h_{\text{STR}}^k|}. \quad (50)$$

According to (46), we have

$$\cos \langle h_{\text{SR}}, h_{\text{STR}}^k \rangle + \cos \langle h_{\text{STR}}^k, h_{\text{SR}} \rangle \geq \gamma |h_{\text{SR}}| |h_{\text{STR}}^k|. \quad (51)$$

Due to the mutuality of angles, we have

$$\theta_k = \angle \langle h_{\text{SR}}, h_{\text{STR}}^k \rangle \leq \arccos \frac{1}{2} \gamma |h_{\text{SR}}| |h_{\text{STR}}^k|. \quad (52)$$

Further, it does not make sense when $\theta_k > \frac{\pi}{2}$ holds, so we have

$$\theta_k \leq \min \left\{ \frac{\pi}{2}, \arccos \frac{1}{2} \gamma |h_{\text{SR}}| |h_{\text{STR}}^k| \right\}, \quad (53)$$

where $\gamma \geq \frac{\exp(W_0(-\exp(-f_{\min})) + f_{\min}) - 1}{|h_{\text{STR}}^k|^2}$. This completes the proof.

REFERENCES

- [1] M. Vaezi *et al.*, "Cellular, wide-area, and non-terrestrial IoT: A survey on 5G advances and the road towards 6G," *IEEE Commun. Surveys Tuts.*, doi: 10.1109/COMST.2022.3151028
- [2] Y. Xu, G. Gui, H. Gacanin, and F. Adachi, "A survey on resource allocation for 5G heterogeneous networks: Current research, future trends, and challenges," *IEEE Commun. Surveys Tuts.*, vol. 23, no. 2, pp. 668–695, 2nd Quart. 2021.
- [3] M. Centenaro *et al.*, "A survey on technologies, standards and open challenges in satellite IoT," *IEEE Commun. Surveys Tuts.*, vol. 23, no. 3, pp. 1693–1720, 3rd Quart. 2021.

- [4] N. Van Huynh *et al.*, "Ambient backscatter communications: A contemporary survey," *IEEE Commun. Surveys Tuts.*, vol. 20, no. 4, pp. 2889-2922, 4th Quart. 2018.
- [5] U. S. Toro, K. Wu, and V. C. M. Leung, "Backscatter wireless communications and sensing in green Internet of Things," *IEEE Trans. Green Commun. Netw.*, vol. 6, no. 1, pp. 37-55, Mar. 2022.
- [6] M. Jin *et al.*, "Parallel backscatter in the wild: When burstiness and randomness play with you," *IEEE/ACM Trans. Netw.*, vol. 29, no. 1, pp. 65-77, Feb. 2021.
- [7] D. Bharadia *et al.* "BackFi: High throughput WiFi backscatter," in *Proc. SIGCOMM*, pp. 283-296, Aug. 2015.
- [8] P. Patel and J. Holtzman, "Analysis of a simple successive interference cancellation scheme in a DS/CDMA system," *IEEE J. Select Areas Commun.*, vol. 12, no. 5, pp. 796-807, Jun. 1994.
- [9] Y. Xu, Z. Qin, G. Gui, H. Gacanian, H. Sari, and F. Adachi, "Energy efficiency maximization in NOMA enabled backscatter communications with QoS guarantee," *IEEE Wireless Commun. Lett.*, vol. 10, no. 2, pp. 353-357, Feb. 2021.
- [10] P. Hu, P. Zhang, M. Rostami, and D. Ganesan, "Braidio: An integrated active-passive radio for mobile devices with asymmetric energy budgets," in *Proc. ACM SIGCOMM*, pp. 484-397, Aug. 2016.
- [11] P. Zhang *et al.*, "Enabling practical backscatter communication for on-body sensors," in *Proc. ACM SIGCOMM*, pp. 370-383, Aug. 2016.
- [12] P. Zhang *et al.*, "Freerider: Backscatter communication using commodity radios," in *Proc. ACM CoNEXT*, pp. 389-401, Nov. 2017.
- [13] D. Li and Y. -C. Liang, "Price-based bandwidth allocation for backscatter communication with bandwidth constraints," *IEEE Trans. Wireless Commun.*, vol. 18, no. 11, pp. 5170-5180, Nov. 2019.
- [14] D. Li, "Capacity of backscatter communication with frequency shift in rician fading channels," *IEEE Wireless Commun. Lett.*, vol. 8, no. 6, pp. 1639-1643, Dec. 2019.
- [15] G. Yang and Y.-C. Liang, "Backscatter communications over ambient OFDM signals: transceiver design and performance analysis," in *Proc. IEEE GLOBECOM*, pp. 1-6, Dec. 2016.
- [16] D. Darsena, "Noncoherent detection for ambient backscatter communications over OFDM signals," *IEEE Access*, vol. 7, pp. 159415-159425, Oct. 2019.
- [17] D. Darsena, G. Gelli, and F. Verde, "Joint channel estimation, interference cancellation, and data detection for ambient backscatter communications," in *Proc. IEEE SPAWC*, pp. 1-5, Aug. 2018.
- [18] Y. Xu, B. Gu, and D. Li, "Robust energy-efficient optimization for secure wireless-powered backscatter communications with a non-linear EH model," *IEEE Commun. Lett.*, vol. 25, no. 10, pp. 3209-3213, Oct. 2021.
- [19] D. Li, "Backscatter communication via harvest-then-transmit relaying," *IEEE Trans. Veh. Technol.*, vol. 69, no. 6, pp. 6843-6847, Jun. 2020.
- [20] D. Li, "Two birds with one stone: exploiting decode-and-forward relaying for opportunistic ambient backscattering," *IEEE Trans. Commun.*, vol. 68, no. 3, pp. 1405-1416, Mar. 2020.
- [21] D. Li, W. Peng, and F. Hu, "Capacity of backscatter communication systems with tag selection," *IEEE Trans. Veh. Technol.*, vol. 68, no. 10, pp. 10311-10314, Oct. 2019.
- [22] Y. Xu, B. Gu, R. Q. Hu, D. Li, and H. Zhang, "Joint computation offloading and radio resource allocation in MEC-based wireless-powered backscatter communication networks," *IEEE Trans. Veh. Technol.*, vol. 70, no. 6, pp. 6200-6205, Jun. 2021.
- [23] Y. Zhang, F. Gao, L. Fan, X. Lei, and G. K. Karagiannidis, "Secure communications for multi-tag backscatter systems," *IEEE Wireless Commun. Lett.*, vol. 8, no. 4, pp. 1146-1149, Aug. 2019.
- [24] D. M. Dobkin, T. Freed, C. Gerdorf, C. Flores, E. Futak, and C. Suttner, "Cooperative tag communications," in *Proc. IEEE RFID-TA*, pp. 27-32, Sept. 2015.
- [25] C. Pérez-Penichet, F. Hermans, and T. Voigt, "On limits of constructive interference in backscatter systems," in *Proc. GIoT*, pp. 1-5, Aug. 2017.
- [26] G. Zheng, M. Wen, Y. Chen, S. Zhao, and H. Du, "Interference exploitation for ambient backscatter communication networks via symbol level precoding," *IEEE Wireless Commun. Lett.*, 2022. doi: 10.1109/LWC.2022.3159777.
- [27] C. Liu, Z. Wei, D. W. K. Ng, J. Yuan, and Y. -C. Liang, "Deep transfer learning for signal detection in ambient backscatter communications," *IEEE Trans. Wireless Commun.*, vol. 20, no. 3, pp. 1624-1638, Mar. 2021.
- [28] Y. Cheng, X. Hua, H. Wang, Y. Qin, and X. Li, "The geometry of signal detection with applications to radar signal processing," *Entropy*, vol. 18, no. 11, p. 381, Aug. 2016.
- [29] T. Van Erven and P. Harremoës, "Rényi divergence and Kullback-Leibler divergence," *IEEE Trans. Inf. Theory*, vol. 60, no. 7, pp. 3797-3820, July 2014.
- [30] Y. Wang, S. Yan, W. Yang, and Y. Cai, "Covert communications with constrained age of information," *IEEE Wireless Commun. Lett.*, vol. 10, no. 2, pp. 368-372, Feb. 2021.
- [31] J. Liu, J. Yu, X. Chen, R. Zhang, S. Wang, and J. An, "Covert communication in ambient backscatter systems with uncontrollable RF source," *IEEE Trans. Commun.*, vol. 70, no. 3, pp. 1971-1983, Mar. 2022.
- [32] W. Chen, H. Ding, S. Wang, and F. Gong, "On the Limits of covert ambient backscatter communications," *IEEE Wireless Commun. Lett.*, vol. 11, no. 2, pp. 308-312, Feb. 2022.
- [33] S. Boyd and L. Vandenberghe, *Convex Optimization*. Cambridge, U.K.: Cambridge Univ. Press, 2004.
- [34] T. Liu, B. Sun, and D. H. K. Tsang, "Rank-one solutions for SDP relaxation of QCQPs in power systems," *IEEE Trans. Smart Grid*, vol. 10, no. 1, pp. 5-15, Jan. 2019.
- [35] Z.-Q. Luo, W.-K. Ma, A. M.-C. So, Y. Ye, and S. Zhang, "Semidefinite relaxation of quadratic optimization problems," *IEEE Signal Process. Mag.*, vol. 27, no. 3, pp. 20-34, May 2010.
- [36] Q. Li, Q. Zhang, and J. Qin, "Secure relay beamforming for SWIPT in amplify-and-forward two-way relay networks," *IEEE Trans. Veh. Technol.*, vol. 65, no. 11, pp. 9006-9019, Nov. 2016.
- [37] G. L. Nemhauser, L. A. Wolsey, M. L. Fisher, "An analysis of approximations for maximizing submodular set functions—I," *Mathematical programming*, vol. 14, no. 3, pp. 265-294, 1978.
- [38] Y. Tao, B. Li, C. Zhao, and Y. -C. Liang, "Hardware-efficient signal detection for ambient backscattering communications," *IEEE Commun. Lett.*, vol. 23, no. 12, pp. 2196-2199, Dec. 2019.
- [39] M. Grant and S. Boyd. (Apr. 2011). *CVX: MATLAB Software for Disciplined Convex Programming*. [Online]. Available: <http://cvxr.com/cvx>.
- [40] F. Chapeau-Blondeau and A. Monir, "Numerical evaluation of the Lambert W function and application to generation of generalized Gaussian noise with exponent $1/2$," *IEEE Trans. Signal Process.*, vol. 50, no. 9, pp. 2160-2165, Sept. 2002.
- [41] D. Li, "How many reflecting elements are needed for energy- and spectral-efficient intelligent reflecting surface-assisted communication," *IEEE Trans. Commun.*, vol. 70, no. 2, pp. 1320-1331, Feb. 2022.